

**FABRICATION AND CHARACTERIZATION OF
POLYVINYL ACETATE SLIME PHANTOM FOR
T1-WEIGHTED, T2-WEIGHTED, AND DIFFUSION
TENSOR MAGNETIC RESONANCE IMAGING**

NURBRANDA CHAW

SCHOOL OF HEALTH SCIENCES

UNIVERSITI SAINS MALAYSIA

2020

**FABRICATION AND CHARACTERIZATION OF POLYVINYL
ACETATE SLIME PHANTOM FOR T1-WEIGHTED, T2-
WEIGHTED, AND DIFFUSION TENSOR MAGNETIC
RESONANCE IMAGING**

by

NURBRANDA CHAW

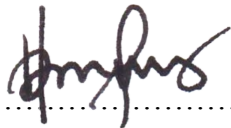
**Dissertation submitted in partial fulfillment
of the requirement for the degree
of Bachelor of Health Science (Honours) (Medical Radiation)**

July 2020

CERTIFICATE

This is to certify that the dissertation entitled FABRICATION AND CHARACTERIZATION OF POLYVINYL ACETATE SLIME PHANTOM FOR T1-WEIGHTED, T2-WEIGHTED, AND DIFFUSION TENSOR MAGNETIC RESONANCE IMAGING is the genuine record of research work by Ms Nurbranda Chaw during the period from February 2019 to July 2020 under my supervision. I have read this dissertation and that in my opinions it conforms to acceptable standards of scholarly presentation and is fully adequate, in scope and quality, as a dissertation to be submitted in partial fulfillment for the degree of Bachelor of Health Science (Honours) (Medical Radiation).

Supervisor,



Dr. Nur Hartini Binti Mohd Taib

Lecturer

Department of Radiology

School of Medical Sciences

Universiti Sains Malaysia, Health Campus

16150 Kubang Kerian, Kelantan.

Date: 20th July 2020

DECLARATION

I hereby declare that the dissertation entitled FABRICATION AND CHARACTERIZATION OF POLYVINYL ACETATE SLIME PHANTOM FOR T1-WEIGHTED, T2-WEIGHTED, AND DIFFUSION TENSOR MAGNETIC RESONANCE IMAGING has been carried out by me in Department of Radiology, Hospital Universiti Sains Malaysia, Kubang Kerian, Kelantan. It is further declared that the dissertation is entirely on the basis of my personal efforts made under the sincere guidance of my supervisor. No portion of the work in this dissertation has been submitted in other institution, if found I shall stand responsible.



.....
NURBRANDA CHAW

Date: 20th July 2020

ACKNOWLEDGEMENT

I would like to express my sincere gratitude for the support I have received from a number of people and organizations. First of all, I would like to thank my main supervisor, Dr. Nur Hartini Binti Mohd Taib for her enthusiasm, patience, insightful observations, helpful knowledge and irresistible ideas, which helped me a lot in my project. I was successfully able to complete this project with her vast knowledge, extensive experience and technical skills in magnetic resonance imaging (MRI). This project would not have been possible without her support and guidance. Throughout my study, I could not have thought that I had a better supervisor that really gives her 100% support.

I would also like to thank to my co-supervisor, Puan Nur Hidayah Yahya Anuar and Hospital Universiti Sains Malaysia (HUSM) for allowing me to collect my data during the movement restriction order (MCO) and give me permission to use the MRI system and equipment at the radiology department, HUSM. Furthermore, I am profoundly thankful to my teammate, Siti Sarah Binti Baharudin for her opinion, suggestion and time during the project progress.

I also want to thank to all my friends especially my classmates that have been accompanied, inspiring and support me during the completion of this project. Above all, I also want to thank my family for the unconditional help they gave and always motivate me towards the completion of this study. They also give financial support during my study and make extra for me to complete this study. Lastly, I am truly grateful for all the above I mentioned and others who helped me a lot to complete this project in a short time.

TABLE OF CONTENTS

CERTIFICATE	ii
DECLARATION	iii
ACKNOWLEDGEMENT	iv
LIST OF TABLES	viii
LIST OF FIGURES	ix
LIST OF ABBREVIATIONS.....	x
ABSTRAK	1
ABSTRACT.....	2
CHAPTER 1 INTRODUCTION	3
1.1 Magnetic Resonance Imaging.....	3
1.2 MRI Phantom.....	4
1.3 Polyvinyl acetate slime.....	5
1.4 Problem statement.....	6
1.5 Objectives.....	7
1.5.1 General objective	7
1.5.2 Specific objectives	7
CHAPTER 2 LITERATURE REVIEW	8
2.1 MRI Phantom.....	8
2.2 Diffusion MRI.....	11
2.2.1 DWI and DTI	12

2.2.2 Phantoms of Isotropic Diffusion	14
2.2.3 Phantoms of Anisotropic Diffusion	15
2.3 3.0 T MRI	16
CHAPTER 3 METHODOLOGY	20
3.1 Materials	20
3.2 Methods	21
3.2.1 Trial phantom and MRI scan	21
3.2.2 Preparation of PVA slime phantom	21
3.2.3 Data acquisition	23
3.2.4 Data analysis	25
3.2.4 a) Characterization of T1, T2, diffusion coefficient and DTI parametric values	25
3.2.4 b) Comparison of relaxation times and diffusion coefficient between all phantoms	27
3.2.4 c) Comparison of relaxation times and diffusion coefficient with those of normal or pathological tissues	28
CHAPTER 4 RESULTS	29
4.1 Results	29
4.1.1 Characterization of T1, T2, and diffusion coefficient	29
4.1.2 Comparison of relaxation times and diffusion coefficient between all phantoms	32

4.1.3 Comparison of relaxation times and diffusion coefficient with those of normal and pathological tissues	34
CHAPTER 5 DISCUSSION	36
CHAPTER 6 CONCLUSION.....	40
6.1 Conclusion.....	40
6.2 Recommendation for future research.....	40
REFERENCES	42
APPENDICES	55
Appendix 1.....	55
Appendix 2.....	59

LIST OF TABLES

Table 1: Parameters of scan protocols.....	9
Table 2: Isotropic diffusion in previous literature.....	14
Table 3: Anisotropic diffusion in previous studies.....	15
Table 4: T1 and T2 readings of swiss mice and ICRC mice.....	17
Table 5: Average T1 and T2 relaxation times at 3.0 T.....	19
Table 6: PVA slime phantoms materials and volume measurements.....	22
Table 7: Parameters for T1WI, T2WI and PDWI.....	24
Table 8: Parameters for diffusion tensor imaging.....	25
Table 9: Type of phantoms as in labeled images A to G.....	29
Table 10: Mean signal intensity of PDWI of all phantoms.....	31
Table 11: Diffusion coefficients of all phantoms with 32 directional resolution.....	31
Table 12: Measured diffusion coefficient (D).....	32
Table 13: approximation of T1 and T2 relaxation times.....	33
Table 14: T1 relaxation times of brain tissues.....	34
Table 15: T1 and T2 relaxation times of healthy human tissues.....	35
Table 16: diffusion coefficient (D) of several human tissues and brain.....	35

LIST OF FIGURES

Figure 1: ACR MRI phantom.....	9
Figure 2: Materials used for the fabrication of the phantoms.....	20
Figure 3: A total of seven phantoms prepared.....	22
Figure 4: Seven phantoms positioned in the head coil at the isocenter of the magnet bore.....	23
Figure 5: A standardized circular region of interest (ROI) on each phantom.....	27
Figure 6: T1WI, T2WI, PDWI and DWI scanned.....	29
Figure 7: Plotted graph of T1 and T2 curves.....	33

LIST OF ABBREVIATIONS

ACR	American College of Radiology
ADC	Apparent Diffusion Coefficient
CN	Caudate Nucleus
CSF	Cerebral Spinal Fluid
CV	Coefficient of Variation
D	Diffusion Coefficient
DTI	Diffusion Tensor Imaging
DWI	Diffusion Weighted Image
EPI	Echo Planar Imaging
FA	Fractional Anisotropy
FOV	Field of View
GM	Gray Matter
MD	Mean Diffusivity
MRI	Magnetic Resonance Imaging
NaCl	Sodium Chloride
NiCl	Nickel Chloride
PCL	Polycaprolactone
PDWI	Proton Density Weighted Image
PVA	Polyvinyl Acetate
PVOH	Polyvinyl Alcohol
QC	Quality Control
RA	Relative Anisotropy
RF	Radiofrequency

ROI	Region of Interest
SE	Spin Echo Sequence
SNR	Signal-to-noise Ratio
T1WI	T1 Weighted Image
T2WI	T2 Weighted Image
TE	Time to Echo
TR	Time to Repeat
TSE	Turbo Spin Echo Sequence
WM	White Matter

ABSTRAK

Fantom slime polivinil asetat (PVA) ialah sejenis perekat yang licin dan likat. Antara kelebihan bahan PVA ialah tidak beracun, murah, tidak kalis air dan mudah untuk disediakan. Tujuan kajian ini adalah untuk mengkaji kebolehan, kesesuaian dan keserasian PVA untuk dijadikan fantom yang boleh menyerupai tisu manusia. Dalam kajian ini, empat fantom slime PVA telah disediakan dengan bahan tambahan yang berbeza iaitu air, minyak, susu dan garam. Penyediaan tiga lagi fantom iaitu air, minyak dan susu digunakan sebagai bahan kawalan. Kesemua tujuh fantom dihasilkan dan dibiarkan pada suhu bilik selama beberapa hari untuk memastikan tiada rongga udara terhasil. Imbasan T1, T2 dan pengimejan tensor difusi dilaksanakan menggunakan sistem MRI Philips Achieva 3 Tesla di Jabatan Radiologi, Hospital Universiti Sains Malaysia (HUSM). Keamatan isyarat dari imej wajaran T1 (T1WI), imej wajaran T2 (T2WI) dan imej wajaran difusi (DWI) bagi kesemua fantom telah diukur. Graf keamatan isyarat melawan TR dan keamatan isyarat melawan TE telah diplot untuk mengetahui nilai masa santaian T1 and T2. Pekali difusi (D) fantom tersebut juga ditentukan berdasarkan pengiraan menggunakan persamaan tertentu. Nilai parametrik DTI bagi kesemua fantom telah direkodkan. Nilai T1, T2 dan D telah dibandingkan dengan tisu manusia yang sihat dan tisu tidak sihat. Dapatan daripada kajian ini menunjukkan lengkung T1 meningkat secara eksponen dengan TR manakala lengkung T2 menurun secara eksponen dengan peningkatan TE. Masa santaian T1, T2 dan juga pekali difusi bagi fantom tertentu menunjukkan ciri-ciri yang sama dengan tisu manusia. Walaubagaimanapun, terdapat artefak hantu diperhatikan dalam T2WI dan DWI yang perlu dihilangkan dalam kajian akan datang. Kesimpulannya, pembikinan fantom slime PVA yang menyerupai tisu manusia untuk kajian MRI adalah sesuai.

ABSTRACT

Polyvinyl acetate (PVA) is a type of adhesive that is squishy and viscous. The advantages of PVA materials are non-toxic, low cost, non-resistant to water and need simple preparation. The aim of the study is to explore the feasibility, suitability, and compatibility of PVA as tissue mimicking phantom for MRI studies. In this study, four PVA slime phantoms were fabricated with different additives that are water, oil, milk, and salt. Three other phantoms were prepared as controls materials that are water, oil, and milk. A total of seven phantoms were prepared and left for several days at room temperature to ensure no air bubbles formed in the phantoms. The T1, T2 and diffusion tensor imaging scan was performed using Philips Achieva 3 Tesla MRI system at the Department of Radiology, Hospital Universiti Sains Malaysia (HUSM). The signal intensity of the T1-weighted images (T1WI), T2-weighted images (T2WI), and diffusion-weighted images (DWI) of all phantoms were measured. Then, graphs of signal intensity vs TR and signal intensity vs TE were plotted to determine the T1 and T2 relaxation times, respectively. The diffusion coefficient (D) of the phantoms was also determined based on calculation using the specific equation. DTI parametric values of all phantoms were also recorded. The T1, T2, and D values were compared with normal and abnormal human tissues. The findings from this study showed that for all phantoms, T1 curves increases exponentially with TR while T2 curves decreases exponentially with increasing TE. The T1 and T2 relaxation as well as diffusion coefficient of the specific phantoms show similar characteristics to some human tissues. However, ghosting artefacts were observed in T2WI and DWI which need to be removed in future studies. To conclude, fabrication of the PVA slime phantom that mimics human tissues for MRI studies are feasible.

CHAPTER 1 INTRODUCTION

1.1 Magnetic Resonance Imaging

There are many types of imaging technologies used for diagnostic purposes. One type of the technology is magnetic resonance imaging (MRI). MRI formed an image of anatomy and physiology of human body. MRI uses non-ionizing radiation which is radio wave that is sent in as the patient is placed in gantry. Signal is emitted from the patient as a result of the change between longitudinal and transversal magnetization after the radio wave is sent in and turned off (Schild, 1990). MRI is safer as it uses non-ionizing radiation instead of ionizing radiation. It also has high spatial and temporal resolution and has a notable ability to differentiate between different types of soft tissues (Yee *et. al.*, 2019).

Diffusion tensor imaging (DTI) is one of the methods used in MRI as a quantitative assessment to map and characterize the diffusion of water within tissues. The image obtained from DTI is due to the molecular random movement of water protons, which produce contrast on the image. Apart from that, DTI images also based on T2 contrast, with adequately long TE (de Souza *et. al.*, 2017). The contrast on high diffusion areas are hypointense while hyperintense on low diffusion areas (Bammer, 2003). This image formed can extract various parametric maps such as fractional anisotropy (FA), relative anisotropy (RA), mean diffusivity (MD) and volume ratio. In clinical applications, the use of DTI is basically increasing due to its technique that is highly sensitive to changes at the cellular and microstructural level (Alexander *et. al.*, 2007). However, the diffusion tensor quantification is affected by the magnetic field, eddy current

compensation, signal-to-noise ratio (SNR) and magnet stability. It requires homogenous magnetic field and eddy current compensation, stable magnet and optimum SNR to obtain good quantification (Wang *et. al.*, 2011).

1.2 MRI Phantom

Phantom is commonly used for quality assurance programme in MRI. Quality assurance programme is done to ensure MRI system is in an optimum condition so that good quality images are produced. MRI phantom should have good signal to noise ratio (SNR), homogeneity, inexpensive, reproducible, mimic human tissues, non-hazardous and the material used should be non-toxic to prevent any harm if contamination occur (Yee *et. al.*, 2019). Besides, the choice of MRI phantom must have same relaxation times and dielectric properties to human tissues and homogenous throughout the phantom, can be fabricated into the shape of human organs chemically and physically stable for a long period of time and strong enough to fabricate a torso without any physical reinforcement (Kato *et. al.*, 2005).

The functions of MRI phantom beside for the usage in quality assurance are to develop new pulse sequences, adjustment of operational conditions, technical training of operators, delineating specific organs and evaluation of safety (Yee *et. al.*, 2019, Hattori *et. al.*, 2013, Ohno *et. al.*, 2008). One of the MRI phantom used for quality control is head phantom from American College of Radiology (ACR), basically used for DTI routine quality control (QC). However, the diffusivity of ACR head phantom used in DTI QC is higher than human brain tissues (Wang *et. al.*, 2011). Furthermore, ACR

head phantom other functions are to perform geometric accuracy test, high-contrast spatial resolution, slice thickness accuracy, slice position accuracy, image intensity uniformity, percent signal ghosting and low-contrast detectability (Ihalainen *et. al.*, 2011). Other than that, fabrication of MRI phantom using a non-toxic material that mimic human tissues has also been introduced for MRI research purposes, such as agarose gel, polyvinyl alcohol slime phantom, polyvinyl alcohol (PVOH) cyrogel phantom, biological phantom using green asparagus and fiber phantoms (Kato *et. al.*, 2005; Latt *et al*, 2007; de Souza *et. al.*, 2017). The polyvinyl alcohol phantom and PVA cyrogel is safe, the values of T1 and T2 are same as the human tissues and its shape can be maintained. However, its stability cannot be confirmed for a long period of time (Mano *et. al.*, 1986; Chu *et. al.*, 1997).

1.3 Polyvinyl acetate slime

Polyvinyl acetate (PVA) is a type of glue or an emulsion adhesive that is squishy and viscous. Two common forms of PVA are organic solvent solution and water dispersion (Ebnesajjad, & Landrock, 2015). It is consisting of non-toxic material that is suitable for the use of phantom fabrication. The viscosity of PVA can be increased when mixed with a cross-linking agent such as borax and then the mixture can form a slime (Yee *et. al.*, 2019). Borax or also known as sodium tetraborate decahydrate ($\text{Na}_2\text{B}_4\text{O}_7 \cdot 10\text{H}_2\text{O}$) is a strong alkaline that can produce boric acid-borate buffer that has an approximately a pH of 9 when hydrolyze in water (Casassa *et. al.*, 1986). The hydrolysis of polyvinyl acetate derives polyvinyl alcohol (PVOH). However, this process is incomplete, which result in the mixture of both polyvinyl acetate and

polyvinyl alcohol (Surry *et. al.*, 2004). PVA and PVOH are both examples of ethylene copolymers. The advantages of PVA that is selected as MRI slime phantom are its material is toxic free, the cost is inexpensive, easily prepared and non-resistant to water. Besides, the characteristics and properties of PVA are suitable to be used under MRI research. It has homogenous and similar relaxation times to human tissues (Yee *et. al.*, 2019).

1.4 Problem statement

There are many benefits of PVA materials such as non-toxic, low cost, water non-resistant and simple preparation as stated in Section 1.3. However, its suitability, compatibility, and the extent to which it has similar intrinsic characteristic with biological tissues such as proton density, magnetic properties and relaxation as well as local magnetic field inhomogeneities needs further investigation. Therefore, the experimental work will be performed using PVA slime to study its potential as tissue mimicking phantom for MRI studies. Study and experiment of new materials and techniques of phantom fabrication are important to make a better phantom for future use.

1.5 Objectives

1.5.1 General objective

The aim of the study is to explore the feasibility, suitability, and compatibility of PVA slime as tissue mimicking phantom for MRI studies.

1.5.2 Specific objectives

1. To fabricate four PVA slime phantoms with different additives (water, oil, salt and milk) as well as prepare three control materials (water, oil and milk)
2. To characterize the T1 and T2 relaxation times as well as the diffusion coefficient of the fabricated phantoms and controls
3. To compare the relaxation times and diffusion coefficient between all preparations and with those of normal or pathological tissues

CHAPTER 2 LITERATURE REVIEW

2.1 MRI Phantom

Magnetic Resonance Imaging (MRI) give out a handy diagnostic image without the use of ionizing radiation and for that, it able to produce images of high quality of the inside part of human body (Haacke *et al.*, 1999). Given the relation between fundamental gene expression patterns with the human anatomy, the functional as well as the progress of imaged tumour are proposed to be asses through quantitative imaging (Gillies *et al.*, 2010).

When compare to imaging methods that uses ionizing radiation, MRI quality assurance are still known to be lacking in some ways. An accredited program from American College of Radiology (ACR) includes standardized images of a phantom as well as protocol for quality measurement (Haacke *et al.*, 1999). Acrylic plastic hollow which being closed at both ends is being used to construct the ACR phantom for MRI. Dimension of the phantom is measured to be 190mm in diameter and 148mm in length. Phantom is filled with about 75 mm of sodium chloride (NaCl) solution as well as about 10 mM of nickel chloride (NiCl₂) solution (American College of Radiology, 1998). The outer part of the phantom is marked with the “NOSE” and “CHIN” words for scanning orientation purpose as if it represents a real head (American College of Radiology, 1998). The phantom is as illustrated in Figure 1 (Etman *et al.*, 2017).



Figure 1: ACR MRI phantom (Etman *et. al.*, 2017).

ACR accreditation program have lined up parameters to be followed for the quality assurance purpose in the use of the ACR phantom. These scan parameters and protocol were obtained with three different scans as in Table 1 below (Kaljuste & Nigul, 2014).

Table 1: Parameters of Scan Protocols (Kaljuste & Nigul, 2014)

Study	ACR Sagittal Locator	ACR Axial T1	ACR Axial T2 double-echo
Pulse sequence	Spin echo	Spin echo	Spin echo
TR (ms)	200	500	2000
TE(ms)	20	20	50
FOV(cm)	25	25	25
Number of slices	1	11	11
Slice thickness(mm)	20	5	5
Slice gap(mm)	-	5	5
NEX	1	1	1
Matrix	256 × 256	256 × 256	256 × 256

The ACR phantom was set to the word “Chin” and “Nose” which represent location of the chin and nose in a standard head study (Etman *et. al.*, 2017). The phantom’s middle part (dark notch) was put in the middle of head coil, then an indicator light aligned the scanner’s isocenter (American College of Radiology, 2000). Accreditation of the phantom consist of 7 test which consist of high-contrast spatial resolution, geometric accuracy, slice thickness accuracy, slice position accuracy, image intensity uniformity, percent signal ghosting and low contrast object detectability (American College of Radiology, 2000).

As it goes for diffusion brain imaging cases, phantom would resemble gray as well as structure of white matter in terms of their anisotropy and diffusivity (Grech-Sollars *et al.*, 2018). Novel type phantom for brain and cardiac which were innovated using electro spun hollow polycaprolactone (PCL), hollow micro-fibers infused with cyclohexane have been reported in the previous studies (Grech-Sollars *et al.*, 2018). Those phantoms have demonstrated an appropriate property of tissue-mimicking and successfully being use in the diffusion MRI validation (Yee *et al.*, 2014; Zhou *et al.*, 2015, 2012; Hubbard *et al.*, 2015; Teh *et al.*, 2016). In fact, brief period of up to 4 months of the reproducibility as well as the stability of the PCL or the phantoms using cyclohexane was also reviewed (Zhou *et al.*, 2012; Teh *et al.*, 2016). Over the period of 1 week, micro-structure of the co-electro spun PCL fiber were particularly remained visibly intact in the cyclohexane (Zhou *et al.*, 2012) while co-efficient of variation (CV) of the apparent diffusion co-efficient (ADC) as well as the FA for the cardiac-mimicking PCL fibers phantom being filled with cyclohexane were discovered to be 1.67% and 2.07% over the period of 4 months (Teh *et al.*, 2016). Despite that, occurrence of hydrolysis for the PCL polymer would most likely happen if the PCL polymer is submerged in a buffered phosphate saline over 3 months period at 37°C

(Bosworth & Downes, 2010). Although the work on degradation of PCL has been acquired in-vivo and in-vitro (Woodruff & Hutmacher, 2010), previous studies on the PCL degradation in cyclohexane remained limited.

2.2 Diffusion MRI

The adoption of model-based diffusion MRI techniques for a large-scale study (Miller *et al.*, 2016) as well as clinical trials (Winston *et al.*, 2014, Mallik *et al.*, 2014) are increasing which increases the need of tissue parameter validation, obtained through diffusion MRI. Validation of obtained metrics from several variation of diffusion MRI methods that ranges from fiber tractography up to size mapping of compartment as well as usage of software phantom (Tournier *et al.*,2002; Leemans *et al.*,2005; Hall & Alexander, 2009; Close *et al.*, 2009; Balls & Frank, 2009), physical phantom (Perrin *et al.*,2005; Fieremans *et al.*,2008; Fillard *et al.*,2011; Farrher *et al.*,2012; Hubbard *et al.*,2015) and ex-vivo samples (Kim *et al.*,2005; Miller *et al.*,2012; Dyrby *et al.*,2011) were taken.

The use of software phantoms would offer a high degree of control with concern to the substrates composition but are limited in terms of the assumption in the synthesis of data and might lacking in realism of the physical tissue (Fan *et al.*, 2018). Ex-vivo sample that comes from actual tissue able to provide genuine tissue's complexity and eventually enables a longer scanning times which certainly not practicable for in-vivo experiment, which results in the wide use of it in the validation of biophysical model (Xu *et al.*, 2014, 2016; Dyrby *et al.*, 2013; Assaf *et al.*, 2008). The process of fixation would alter physical properties of the tissue up until the composition of sample might

not accurately reflected in the in-vivo properties (Fan *et al.*, 2018). Ex-vivo tissue samples known to undergo alterations which reflected in diffusion MRI experiments such as low fractional anisotropy (Shepherd *et al.*, 2009a), low diffusivity (McNab *et al.*, 2009; Sun *et al.*, 2005) compartment changes (Shepherd *et al.*, 2009b), and disfiguration of tissue and shrinkage (Wehrl *et al.*, 2015). Some of the limitations of the physical phantoms which mimic biological tissues mentioned above might be overcome through a simplified representation (Fan *et al.*, 2018).

2.2.1 DWI and DTI

Microscopic features of the water molecules diffusion throughout and in between biological tissues are revealed by the diffusion-weighted imaging (DWI) (Moseley *et al.*, 1990). These images show a contrast which based on the water photon's random motion on a molecular level (Souza *et al.*, 2017). Diffusion process in a biological tissue are known to be either anisotropic (follows specific direction) and isotropic (magnitude is same in all directions) (Souza *et al.*, 2017). Acquisitions of DWI involves application gradients of diffusion-weighting in pulse sequences which eventually creates an attenuation of signal because of the water photon's microscopic motion (Souza *et al.*, 2017). Clinical practices show DWI ability to identify acute stroke at when the symptoms start to take place and classifying it as non-ischemic or ischemic while the rest imaging techniques just shows brain changes after onset is taking place. The DTI images as well as the ADC or Apparent Diffusion Coefficient can be retrieved through DWI images. The measured values in ADC maps are lower when compared to the one being observed when free water diffusion take place (no compartments interference and barriers acquired in the biological tissues) (Souza *et al.*, 2017).

In pulse sequence diffusion, echo time (TE) have to be long enough for it to be match or compatible with diffusion gradient's that, the images of DWI are also viewed depending on the T2 contrast. Areas with higher diffusion are typically known to be hypo-intense while those with lower diffusion areas are known to be hyper-intense in the DW images (Bammer, 2003). The tensor model shows the DTI principle in which described as multivariate Gaussian distribution with a 3×3 co-variance matrix as in equation 1 (Souza *et al.*,2017):

$$T = \begin{pmatrix} D_{xx} & D_{xy} & D_{xz} \\ D_{yy} & D_{yx} & D_{yz} \\ D_{zz} & D_{zx} & D_{zy} \end{pmatrix} \quad (\text{Equation 1})$$

The matrix above explains that the three dimension water molecules displacement is normalized by diffusion time and that diagonal elements above are the variances for diffusion along the x, y and z axes while the off-diagonal are terms for the symmetrical co-variance (Souza *et al.*,2017). Given the tensor symmetry, it can also be viewed as an image and technique of obtaining the DWI images in a few directions in order to construct tensor known as diffusion tensor imaging or DTI (Basser, 1997). The DTI image makes it possible to extract scalar parameters such as the fractional anisotropy (FA), mean diffusivity (MD), relative anisotropy (RA) and the volume ratio (Souza *et al.*, 2017).

The accuracy of the DWI and DTI are dependent on the accuracy of the acquired data. The lower the SNR, chemical shift, patient's movement during scanning process, in-homogeneity of magnetic field, eddy current, RF interference and effects of the

magnetic susceptibility are able to demean the quality of images for DWI and DTI (Le Bihan *et al.*, 2006). Recently, multiple studies have suggested the use for quality control (QC phantoms with acquisitions of diffusion which are based on different type of materials as well as of geometrical variation (Teh *et al.*,2016; Hubbard *et al.*,2015; Hellerbach *et al.*, 2013; Fieremans *et al.*, 2008).

2.2.2 Phantoms of Isotropic Diffusion

Usually, the isotropic phantoms come in cylinder, spheres or in the shape of tube that is filled with gels or liquids of which relaxation or its properties of diffusion are likely to be similar with biological tissues in MRI surroundings. Previous studies with regards of isotropic diffusion phantom, agarose or agar is the most applied one of all compounds. Table 2 below shows summarization of isotropic phantom's characteristic from previous literature (Souza *et al.*, 2017):

Table 2: Isotropic diffusion in previous literature

Reference	Phantom	Maximum b-value (s/mm ²)	ADC (Mean ± Standard Deviation) (mm ² /s)
Gatidis <i>et al.</i>, (2014)	PEG filled tubes and different concentrations of gadobutrol	1000	Ranges: 500,800,1200 and 2000
Boursianis <i>et al.</i>, (2014)	Polyacrylamida gel with sucrose solution filled tubes of different concentrations	1000	Not showed
Lavdas <i>et al.</i>, (2013)	Gels filled compartment of spherical phantom (agarose/sucrose concentrations differ)	1000	$(1.91 \pm 0.02) \times 10^{-3}$
Kato <i>et al.</i>, (2005)	CAGN and GAG compounds		Not calculated

2.2.3 Phantoms of Anisotropic Diffusion

Phantoms of anisotropic diffusion are very helpful for the QC of DTI. The DTI phantom was being made from layers of isotropic gel with agar-based and each of the layer have different conductivity (Souze *et al.*, 2017). It has also been revealing that gels would make a firmer setup and help to decrease artifact's imaging causes by a decrease in macroscopic water reflux. Table 3 below shows the summarization from previous literature for anisotropic diffusion.

Table 3: Anisotropic diffusion in previous studies

Reference	Phantom	Maximum b-value (s/mm ²)	Maximum NDGD	Maximum MD or (Mean ± Standard Deviation) (mm ² /s)	Maximum FA or (Mean ± Standard Deviation)
Kim <i>et al.</i> , (2016)	Distilled water filled capillary (sealed)	2000	15	(1.74 ± 0.07)	(0.23 ± 0.05)
Teh <i>et al.</i> , (2015)	PCL and PEO filled plastic syringe	2000	30	(7.53 ± 0.16) × 10 ⁻⁴	(0.388 ± 0.007)
Hubbard <i>et al.</i> , (2015)	PCL fibers in glass tube	800	30	(3085 ± 0.5) × 10 ⁻³ (6.61 ± 0.6) × 10 ⁻³	0.45 ± 0.5
Hellerbach <i>et al.</i> , (2013)	Cylindrical poly-amide spindle surround by poly-ester fiber in water	700	30	Measure of signal intensity	
Lorenz <i>et al.</i> , (2008)	Material testing for phantoms construction (viscose, linen, rayon, polyamide, hemp and Dyneema)	1000	61	(1.4 ± 0.2) × 10 ⁻³ Polyamide (1.1 ± 0.1) × 10 ⁻³ Dyneema	(0.3 ± 0.1) polyamide (0.63 ± 0.1)

2.3 3.0 T MRI

The SNR in MRI give out the function of the main magnetic field strength, volume of tissue that is being imaged as well as the radio frequency of the coil that is being used. Many of the conventional MRI of musculoskeletal system is being done at 1.5 T, but it is becoming most prevalent to use system of higher field strength as 3.0 T (Gold *et al.*, 2004). Due to the linearity between available magnetization and field strength, the 3.0 T imaging able to deliver twice of the intrinsic SNR imaging at 1.5T if both the subject and coils are equivalent to one another (Collins & Smith, 2001). On the other hand, The SNR benefit at 3.0T may be limited due to changes of field-dependent in the tissue's relaxation time as well as the difference in chemical shift between water and fat (Gold *et al.*, 2004). There would be a slight decrease of the spin-spin relaxation time T2 at higher field-strength but fairly constant at different field-strength (Bottomley *et al.*, 1984). Meanwhile, spin lattice relaxation time T1 shows an increase when there is an increase of the field-strength.

The dissimilarities between relaxation time of malignant and normal tissues are proposed to mainly cause by higher tissue hydration faced by the malignant tissues (Kiricuta & Simplaceanu, 1975). It was countered after the difference in water content between the cancer cells and normal cells was calculated to be less than 10% which cannot be held accountable for the dissimilarities of relaxation times between the two cells (Ling & Tucker, 1980). Past research reported in a study that uses ICRC mice and Swiss mice gave out reading of T1 and T2 as shown in Table 4 (Shah *et al.*, 1982). The inconsistencies of the water content value throughout the previous study shows that the mechanism of relaxation times is still debated and in need of further studies.

Table 4: T1 and T2 readings of Swiss mice and ICRC mice (Shah et al., 1982).

	Swiss Mice				ICRC Mice			
	Normal Tissue		Tissue with Tumor		Normal Tissue		Tissue with Tumor	
	T1 value (ms)	Water content (%)	T1 value (ms)	Water content (%)	T1 value (ms)	Water content (%)	T1 value (ms)	Water content (%)
Liver	426 ± 12	70.8 ± 0.25	615 ± 17	72.5 ± 0.42	375±29	68.8±2.4	366±17	70.8± 0.75

Basic parameters that lies behind the MRI are based on the value of relaxation times of T1 and T2 (Bojorquez *et al.*, 2016). Therefore, efforts have been done into validating and developing measurement methods as well as to collect relaxation times value at different magnetic fields for different type of tissues such as abdominal, musculoskeletal, pelvic and brain tissue (Tofts & du Boulay, 1990). Hence, the accurate knowledge on the tissue relaxation times serve as an important feature for the optimization and the development of the MR sequences (Edden *et al.*,2010). In addition, tissue relaxation times are able to serve a possibility of computing pure relation maps of T1 and T2 which its contrast is mainly based on T1 or T2 respectively (Bojorquez *et al.*, 2016). The relaxation maps would allow the performing of quantitative imaging such as volume and blood perfusion as well as evaluation of iron overload and contrast agent uptake which are most definitely not comprehensible in the conventional qualitative weighted imaging of T1 and T2 (Bojorquez *et al.*, 2016).

In the weighted images of T1 and T2, contrast of the images is not only due to the differences in relaxation times of T1 and T2 but also based on the intrinsic and myriad extraneous factors (eg. density of proton, gain effects, radio frequency (RF) field and sensitivity of coil receiver (Ma *et al.*, 2013; Wright *et al.*, 2008; Deoni *et al.*, 2006). A

tissue state marker of higher reliability is being provided as the relaxation times does not dependent towards these factors (Wright *et al.*, 2008) and this serve as an important property in the studies of the tissue pathology (Stanisz *et al.*, 2005). In a case where the tissues might own a specific value of its relaxation times, the tissues could be classified and segmented with accordance the values obtained (Bojorquez *et al.*, 2016). Despite that, the wide range of values being reported through the previous studies often refuted one another, which possibly due to the inconsistency and measurement methods being used. The use of distinctive sequences and hardware differences (Rakow-Penner *et al.*, 2006). As an example, the reported values of T1 at 3.0 T for white matter ranges between 699 up to 1735 ms (Bojorquez *et al.*, 2016).

Besides, the selection of the parameters for image pulse sequence are directly being affected by the T1 and T2 which would affect the entire imaging times and eventually patient's throughput (Duewell *et al.*, 1996). The T1 and T2 relaxations times are identified to modified significantly with field strength, yet these changes would be determined by mobility of water and other tissue properties, making it hard to be predicted accurately using theoretical calculation. Previous study has reported of such values for brain (Wansapura *et al.*, 1999), but less are known for body tissues. In a study which involve 6 healthy adults of three men and three women, the T1 and T2 relaxation times reading for abdominal as well as public tissues which measured in an in-vivo manners at 3.0 T are in Table 5 (de Bazelaire *et al.*, 2004).

Table 5: Average T1 and T2 relaxation times at 3.0 T

Tissue	T1 relaxation time (ms)*	R² value (%)	T2 relaxation time (ms)*	R² value (%)
Kidney				
-Cortex	1,142±154	0.990	76±7	0.993
-Medula	1545±142	0.999	81±8	0.996
Liver	809±71	0.987	34±4	0.984
Spleen	1328±31	0.998	61±9	0.996
Pancreas	725±71	0.976	43±7	0.977
Paravertebral muscle	898±33	0.988	29±4	0.867
Bone marrow (L4 vertebra)	586±73	0.994	49±4	0.994
Subcutaneous fat	382±13	0.999	68±4	0.999
Uterus				
-Myometrium	1514±156	0.999	79±10	0.993
-Endometrium	1453±123	0.998	59±1	0.999
-Cervix	1616±61	0.998	83±7	0.992
Prostate	1597±42	0.998	74±9	0.995

*Data are mean ± SD

CHAPTER 3 METHODOLOGY

3.1 Materials

The chemicals used in this study are as follows: polyvinyl acetate (PVA) (Q-Stationers Sdn. Bhd), sodium tetraborate or borax with molecular formula $[\text{Na}_2\text{B}_4\text{O}_7 \cdot 10\text{H}_2\text{O}]$ (Doozie, Mondo Marketing Sdn. Bhd), distilled water, oil, salt (Adabi Consumer Industries Sdn. Bhd), milk (Dutch Lady® Milk Industries Bhd), as shown in Figure 2 (A-D). The apparatus used are plastic container, stirrer, 12 cc and 15 cc syringes, thermometer and MH-Series pocket weighing scale. The MRI system used was a 3T Philips Achieva TX, Philips Healthcare, Best, The Netherlands.



Figure 2: Materials used for the fabrication of the phantoms.

3.2 Methods

3.2.1 Trial phantom and MRI scan

The experimental work was started with preparing a set of phantoms and performing trial MRI scan, as shown in Appendix 1 (Table I – VI and Figure I).

3.2.2 Preparation of PVA slime phantom

Four types of PVA slime phantom were fabricated with different types of chemicals, which are PVA with borax and distilled water, PVA with borax and oil, PVA with borax and salt and PVA with borax and milk. Three materials were prepared as a control for this study, which are distilled water, oil and milk. Hence, there are total of 7 phantoms prepared for this study as shown in Figure 3.

All phantoms were prepared according to the following steps: 1g of borax powder was weighted using a pocket weighting scale and was dissolved in 100 ml of warm water at a temperature of 80-90°C. Dissolved borax powder was left in the room temperature. 20 ml of PVA and 5 ml of 1% concentration borax was added into four different containers. 2 ml of distilled water, oil, 25% concentration salt and milk were added into the containers. All the solution in the containers were stirred slowly to form PVA slime phantom. The borax reacted completely with the PVA solution to form slime phantom. Another three containers were prepared as a control. The volume for milk, oil

and water are 20 ml for each. The volume of all materials was measured using 12 cc and 25 cc syringes. All the phantom prepared were stored at room temperature for at least a week to ensure no air bubbles present in the slime phantom. Table 6 shows the details about the quantity of the ingredients used to form the PVA slime phantom.

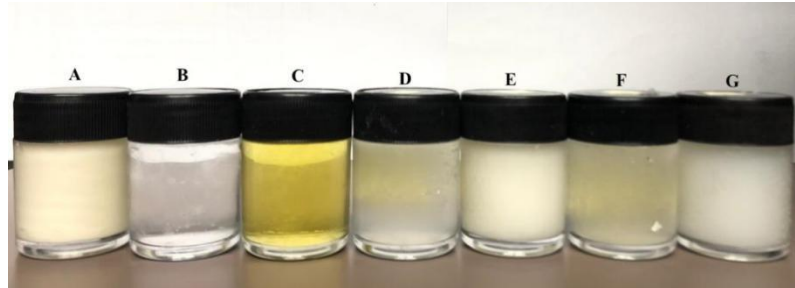


Figure 3: A is milk, B is distilled water and C is oil. A – C are the control materials in this study. D is PVA slime phantom with distilled water, E is PVA slime phantom with oil, F is PVA slime phantom with 25% concentration of salt and G is PVA slime phantom with milk

Table 6: PVA slime phantom ingredients and volume measurements

Sample	Solution	Volume of PVA solution (ml)	Volume of Borax solution (ml)	Concentration of Borax solution (gml^{-1})	Volume of the other mixture (ml)
1	Milk	-	-	-	-
2	Water	-	-	-	-
3	Oil	-	-	-	-
4	PVA + Borax + Water	20	5	0.01	2
5	PVA + Borax + Oil	20	5	0.01	2
6	PVA + Borax + Salt	20	5	0.01	2 (25% concentration of salt)
7	PVA + Borax + Milk	20	5	0.01	2

3.2.3 Data acquisition

Data were acquired using Philips Achieva 3 Tesla MRI system Philips Healthcare, Best, The Netherlands at the Department of Radiology, Hospital Universiti Sains Malaysia (HUSM). All seven phantoms were positioned in the head coil at the isocenter of the magnet bore and scanned simultaneously, as shown in Figure 4.

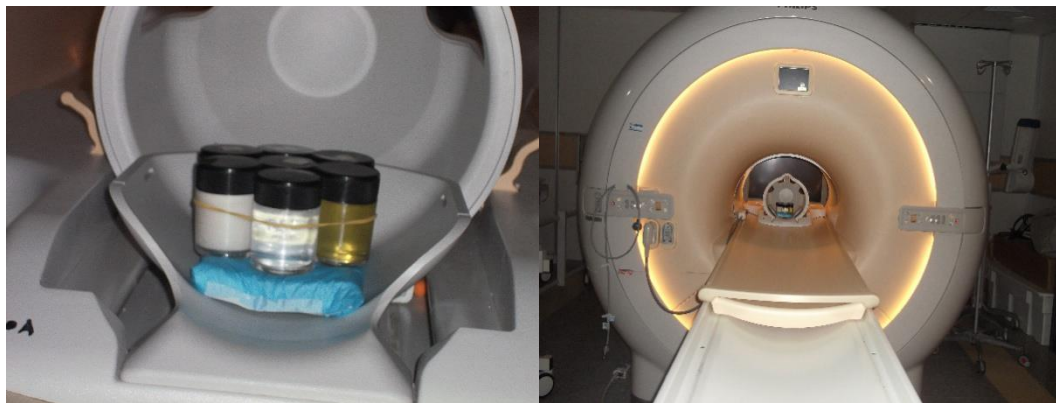


Figure 4: Seven phantoms positioned in the head coil at the isocenter of the magnet bore

MR images were acquired using spin echo (SE) pulse sequence for coronal T1WI, turbo spin echo (TSE) pulse sequence for coronal T2WI, turbo spin echo (TSE) coronal proton density and echo planar imaging (EPI) for diffusion tensor imaging. The parameters used for T1 are constant TE = 10 ms and variables TR = 100, 300, 500, 700, 900, 1100, 1300, 1500, 2000, 2500, 3000, 3500, 4000, 4500 and 5000 ms. Parameters for T2 are, constant TR = 3000 ms and variables TE = 22.28, 30, 50, 70, 90, 110, 130, 150, 170, 190, 210, 230, 250, 270, and 300 ms and parameters for proton density is TE = 30 ms and TR = 2500 ms. Other parameters for both images acquired are 1 slice of 3 mm slice thickness with no gap, field of view (FOV) = 230 × 183 mm, matrix size for

T1 is $0.90 \times 1.12 \times 3.0$, T2 is $1.55 \times 1.95 \times 3.00$ and proton density is $0.4 \times 0.42 \times 3.00$, as shown in Table 7. Diffusion tensor imaging using 32 directional resolution, TE = 73 ms, TR = 1119 ms which is the shortest TR for DWI, 10 slices were imaged with 2.5 mm slice thickness, FOV = 240×180 mm and b-value = 0 for baseline image (T2) and b-value = 1000 for DWI, as shown in Table 8. The DWI images were acquired in 32 directions to improve the accuracy in tensor estimation (de Souza *et. al.*, 2017).

All images were saved and transferred to an independent workstation for data analysis. Mean signal intensity and standard deviation for each PVA slime phantom images and controls from the saved images were recorded by setting a circularly shaped region of interest (ROI) on the image.

Table 7: Parameters for T1WI, T2WI and PDWI

Images	Sequence	TE (ms)	TR (ms)	Slice thickness	Slice	Gap	FOV
Coronal T1WI	Spin echo	10	100, 300, 500, 700, 900, 1100, 1300, 1500, 2000, 2500, 3000, 3500, 4000, 4500, 5000				
Coronal T2WI	Turbo spin echo	22.28, 30, 50, 70, 90, 110, 130, 150, 170, 190, 210, 230, 250, 270, 300	3000	3 mm	1	0	230 × 183
Coronal PDWI	Turbo spin echo	30	2500				